DEUTSCHES ELEKTRONEN-SYNCHROTRON DESY

DESY 82-073
November 1982

RECENT RESULTS FROM TASSO AT PETRA

by

TASSO Collaboration

Presented by

Dieter Lüke

NOTKESTRASSE 85 · 2 HAMBURG 52

To be sure that your preprints are promptly included in the
HIGH ENERGY PHYSICS INDEX ,
send them to the following address (if possible by air mail) :

DESY
Bibliothek
Notkestrasse 85
2 Hamburg 52
Germany

DESY 82-073
November 1982

RECENT RESULTS FROM TASSO AT PETRA

TASSO Collaboration

Talk given at the XXI International Conference on
High Energy Physics, Paris, 26 - 31 July, 1982

by

Dieter Lüke
DESY, Hamburg

1. Spectra of identified charged particles[1)]

The spectra of the charged particles $\pi^\pm$, $K^\pm$, $p(\bar{p})$ and Λ ($\bar{\Lambda}$) have been measured over a wide range of momenta. The particles were identified by time-of-flight systems and by Cerenkov counters. The integrated luminosities and numbers of hadronic events collected at various c.m. energies W are given in the following table.

W (GeV)	$\int$Ldt (nb^{-1})	hadronic events
12 - 14	1720	2962
22 - 30	3200	2289
30 - 36.7	80312	22388

In Fig. 1 we show the fraction of charged $\pi^\pm$, $K^\pm$, and $p(\bar{p})$ among all charged hadrons as a function of momentum. At particle momenta of 0.4 GeV/c more than 90% of the charged hadrons are pions. With increasing momentum the fraction of $\pi^\pm$ among the charged hadrons decreases while the fractions of $K^\pm$ and $p(\bar{p})$ are increasing. At W = 34 GeV and a momentum of 5 GeV/c the particle fractions are approximately $\pi^\pm : K^\pm : p(\bar{p}) = 0.55 : 0.3 : 0.15$. In Fig. 2 the average multiplicity of $\pi^\pm$, $K^\pm$, $p(\bar{p})$ and $\Lambda(\bar{\Lambda})$ is shown as function of W. The yield of $p(\bar{p})$ is rising faster with W than that of $\pi^\pm$ and $K^\pm$. At W = 34 GeV the ratio $p(\bar{p}) : \pi^\pm$ is twice as large as at W = 5 GeV. On average an event at W = 34 GeV contains 10.3 ± 0.4 $\pi^\pm$, 2.0 ± 0.2 $K^\pm$, 0.8 ± 0.1 $p(\bar{p})$ and 0.33 ± 0.04 Λ ($\bar{\Lambda}$). Note that in both figures the $\pi^\pm$ spectra include particles from K^0_S decay, the $p(\bar{p})$ spectra include particles from hyperon decay (like $\Lambda,\bar{\Lambda}$).

We measured also inclusive ρ^0 production[2)]. Assuming ρ^0, ρ^+, ρ^- to have equal production rates we find that $\approx 30\%$ of all $\pi^\pm$ result from ρ decay.

2. Scale breaking in inclusive charged particle production[3)]

The scaled cross section $sd\sigma/dx_p$ (with $x_p = p/E_{beam}$) for inclusive charged particle production is shown in Fig. 3 for c.m. energies between 12.0 and 36.7 GeV. Scale breaking is observed. For $x_p > 0.2$ the cross

section decreases by ≈ 20% when W increases from 14 to 35 GeV. When parametrizing the s-dependence of the scaled cross section as $\sim 1 + c_1 \ln (s/1GeV^2)$ a fit yields the curves shown in Fig. 3. The values of c_1 are given in Fig. 4, together with similar results obtained by the PLUTO experiment.

3. $D^{*\pm}$ production

Production of charmed hadrons is of special interest since charmed hadrons (as well as bottom hadrons) contain the primary charm quark (resp. bottom quark). That is because at PETRA energies (for our data sample W ≈ 32 GeV) production of charmed and bottom hadrons from the sea is negligible. We determined the cross section for inclusive $D^{*\pm}$ production and its production angular distribution in a search for electromagnetic-weak interference effects in charm quark pair production. D^{*+} were identified through the decays $D^{*+} \to D^0\pi^+$ (branching ratio 44 ± 10%) and $D^0 \to K^-\pi^+$ (branching ratio 3.0 ± 0.6%). Fig. 5 shows the distribution of the mass difference $\Delta M = M(K^-\pi^+\pi^+) - M(K^-\pi^+)$ for $M(K^-\pi^+)$ masses in the D^0 mass region (1.74 - 1.98 GeV) and for high energetic D^{*+} with fractional energy $x = E_{K^-\pi^+\pi^+} / E_{beam} > 0.5$, assuming each particle in turn to be a kaon and a pion. The decay $D^{*+} \to D^0\pi^+$ is indicated by the narrow peak centered around $\Delta M = 0.145$ GeV. Its width agrees with the expected rms resolution of about 1.5 MeV. Fig. 6 shows the scaled cross section $s \cdot d\sigma/dx$ for inclusive $D^{*\pm}$ production, after correcting for decays other than $D^{*+} \to D^0\pi^+$ and $D^0 \to K^-\pi^+$. The production angular distribution of $D^{*\pm}$ (Fig. 7) is asymmetric. A fit to the form $1 + a\cos\theta + \cos^2\theta$ (where parameter a is fitted) yields an asymmetry of $A = -0.35 \pm 0.14$. For comparison, an asymmetry of about -0.14 is expected for production of charm quarks.

Provided statistics can be improved in the future, the study of $D^{*\pm}$ production will allow to measure the weak neutral coupling of the charm quark.

4. Neutral weak current effects[4)]

Electroweak interference effects have been studied in lepton pair production $e^+e^- \to e^+e^-$, $\mu^+\mu^-$, $\tau^+\tau^-$. Fig. 8 shows the measured differential cross sections at an average W = 34.4 GeV, normalized to the QED cross

section. In case of $\mu^+\mu^-$ production an asymmetric angular distribution is seen. The measured forward-backward charge asymmetries $A_{\mu\mu}$ and $A_{\tau\tau}$ are given in the following table together with the values A_{GWS} expected from the standard GWS theory.

	EVTS	nb^{-1}	$A_{measured}$	A_{GWS}	$\lvert\cos\theta\rvert$
$\mu^+\mu^-$	2391	70200	-0.104±0.023	-0.092	≤ 1.0
$\tau^+\tau^-$	577	65800	-0.056±0.044	-0.080	≤ 0.8

The data have been corrected for higher order QED processes. The measured asymmetry $A_{\mu\mu} = -0.104 \pm 0.023$ is in good agreement with the value -0.092 expected from GWS theory. Within the GWS theory a combined fit to the e^+e^- and $\mu^+\mu^-$ cross sections gave $\sin^2\theta_W = 0.27\ ^{+0.06}_{-0.07}$. Assuming $M_Z = 90$ GeV, a fit of the vector and axial-vector couplings resulted in $g_v^2 = -0.04 \pm 0.06$, $g_a^2 = 0.26 \pm 0.07$. This is in good agreement with the prediction of the GWS theory: $g_v^2 = 0.25\ (1 - 4\sin^2\theta_W)^2 = 0.0016$ for $\sin^2\theta_W = 0.23$, and $g_a^2 = 0.25$. If we fix $g_v^2 = 0.0016$ and $g_a^2 = 0.25$, we can fit for the mass of the Z^0 : the 95% confidence limits are 46 GeV < M_Z < 155 GeV.

5. Hadronic cross section $\sigma(e^+e^- \to \text{hadrons})$[5)]

The ratio $R = \sigma(e^+e^- \to \text{hadrons}) / \sigma_{\mu\mu}$ was measured for c.m. energies W between 12.0 and 36.7 GeV with a precision of typically ±5.2%. The error includes a systematic error of ±2% for higher order ($> \alpha^3$) QED corrections. For W > 14 GeV, R is constant with an average R = 4.[illegible] ± 0.03 (stat) ± 0.20 (syst). Quarks are found to be pointlike with a mass-parameter describing a possible quark formfactor: $\Lambda_+ > 186$ GeV. A comparison with R values from other PETRA experiments is done by Heinzelmann[6)].

6. Search for charged Higgs and technipions[7)]

We have searched for charged Higgs mesons and technipions (denoted as H^{+-}) in the process $e^+e^- \to H^+H^-$. While the leptonic decay $H \to \tau\bar{\nu}_\tau$ for masses M_H = 4 - 13 GeV had been excluded by other experiments[8)], we studied the pro-

cess where both H decay into hadrons: $H^+ \to c\bar{s}$ and $c\bar{b}$. From our sample of 20000 hadronic events (corresponding to a total integrated luminosity of 71.5 pb^{-1} at c.m. energies between 33 and 37 GeV) we find that production of charged Higgs and technipions is excluded (with 95% c.l.) in the mass range 5 - 13 GeV and for hadronic branching ratios larger than about 70% for the decay $H^+ \to c\bar{s}$ and $c\bar{b}$ (see Fig. 9), provided $BR(H \to c\bar{b}) / BR(H \to c\bar{s}) < 0.5$ as expected by theory. In Fig. 9 our result is shown together with the JADE result. Taken together, the two experiments exclude the existence of a pointlike charged scalar particle, with decay modes as discussed, in the mass range between 5 and 13 GeV.

7. Leptonic decays of b-quarks

From a study of inclusive $\mu^{\pm}$ and $e^{\pm}$ spectra from hadronic events at c.m. energies around 34.6 GeV we obtained the branching ratios:

$$BR(b \to \mu\nu X) = 15.0 \pm 3.5 \text{ (stat.)} \pm 3.5 \text{ (syst.)} \%, \text{ and}$$
$$BR(b \to e\nu X) = 13.6 \pm 4.9 \text{ (stat.)} \pm 4.0 \text{ (syst.)} \%.$$

The forward-backward charge asymmetries of the leptons were determined to $A(\mu) = -0.17 \pm 0.10$ and $A(e) = -0.11 \pm 0.17$, compared to an asymmetry of -0.084 as expected from GWS theory.

8. Radiative width of f'(1515)[9]

In photon-photon collisions we observed the excitation of the f'(1515) and its decay into K^+K^- (Fig. 10a) and into $K^0_S K^0_S$ (Fig. 10b). Assuming the f' is produced in a helicity = 2 state, we determined the product of radiative width times branching ratio for the decay into $K\bar{K}$: $\Gamma(f' \to \gamma\gamma) \cdot BR(f' \to K\bar{K}) = 0.11 \pm 0.02$ (stat.) $\pm$ 0.04 (syst.) keV. The decay $f' \to K\bar{K}$ is dominant. Using the limits $0.5 < BR(f' \to K\bar{K}) < 1$ and the radiative width of the f^0 meson, $\Gamma(f^0 \to \gamma\gamma) = 2.95 \pm 0.40$ keV (Ref.10) we estimated the mixing angle θ of the $J^{PC} = 2^{++}$ nonet within the framework of SU(3) to be within the 95% confidence limits: $25.4^0 < \theta < 34.7^0$. This agrees with the value $\theta = 28^0 \pm 3^0$ obtained from the quadratic Gell-Mann Okubo mass formula. The small radiative width $\Gamma(f' \to \gamma\gamma)$ constrains the fraction of non-strange quarks in f' to be < 3% (95% c.l.).

9. Observation of a narrow structure at 2.1 GeV in $\gamma\gamma \to \pi^+\pi^-\pi^+\pi^-$

A narrow structure has been observed in the four pion system of the reaction $\gamma\gamma \to \pi^+\pi^-\pi^+\pi^-$. The data correspond to a total integrated luminosity of about 84 pb^{-1}, most of them taken at a beam energy of 18.3 GeV. The exclusive $\pi^+\pi^-\pi^+\pi^-$ channel was separated from events with additional, undetected particles by requiring a low net momentum transverse to the beam: $|\Sigma \vec{p}_T| < 0.070$ GeV/c. Assigning pion masses to all particles there are a total of 3955 events with a $\pi^+\pi^-\pi^+\pi^-$ mass $M_{4\pi} < 4$ GeV. The $M_{4\pi}$ mass distribution (Fig. 11) shows a narrow structure near 2.1 GeV. A smooth background of the shape $(a + b \cdot M) \cdot \exp(-c \cdot M)$ was fitted to the data between 1.65 and 3.00 GeV, including the signal region near 2.1 GeV. In the mass interval 2.05 - 2.15 GeV the fit predicts 190 $\pm$ 14 events, whereas 250 events are observed. This deviation from the smooth curve corresponds to an effect of 4.3 standard deviations. Interpreting the structure as a resonance we fitted a non-relativistic Breit-Wigner shape plus a smooth background to the data, folding the Breit-Wigner with a Gaussian distribution in order to account for our mass resolution ($\sigma \approx 25$ MeV). The fit gave $M_0 = 2.100 \pm 0.020$ GeV for the mass (the error includes a systematic uncertainty of 0.020 GeV), $\Gamma = 0.030 \pm 0.034$ GeV for the width of the Breit-Wigner, and $N_0 = 97 \pm 40$ events under the Breit-Wigner curve. After correcting for acceptance (which is 4% on average) the coupling strength to $\gamma\gamma$ is determined to $\Gamma_{\gamma\gamma} = [1.25 \pm 0.5 \text{ (stat.)} \pm 0.5 \text{ (syst.)}] / (2J + 1)$ (keV) where J is the spin of the assumed resonance.

References:

1. TASSO Collaboration, M.Althoff et al., DESY-Report No. 82-070 (1982).
2. TASSO Collaboration, R.Brandelik et al., DESY-Report No. 82-046 (1982).
3. TASSO Collaboration, R.Brandelik et al., Phys.Lett. 114B (1982) 65.
4. TASSO Collaboration, R.Brandelik et al., DESY-Report No. 82-032 (1982).
5. TASSO Collaboration, R.Brandelik et al., Phys.Lett. 113B (1982) 499.
6. G.Heinzelmann, contribution to this conference.
7. TASSO Collaboration, M.Althoff et al., DESY-Report No. 82-069 (1982).
8. JADE Collaboration, W.Bartel et al., Phys.Lett. 114B (1982) 211,
   CELLO Collaboration, H.J.Behrend et al., DESY 82-021 (1982),
   MARK J Collaboration, A.Adeva et al., LNS Technical Report Number 125 (1982),
   MARK II Collaboration, C.A.Blocker et al., SLAC-PUB-2923 (1982).
9. TASSO Collaboration, M.Althoff et al., DESY-Report No. 82-071 (1982).
10. Particle Data Group, Phys.Lett. 111B (1982) 1.

Figure Captions:

Fig. 1 Inclusive charged particle production. Fraction of $\pi^{\pm}$, $K^{\pm}$, $p(\bar{p})$ as function of particle momentum at c.m. energies W = 14, 22 and 34 GeV.

Fig. 2 Inclusive charged particle production. Averaged multiplicity of $\pi^{\pm}$, $K^{\pm}$, $p(\bar{p})$, and Λ ($\bar{\Lambda}$) as function of c.m. energy.

Fig. 3 Inclusive charged particle production. Scaled cross section $s\, d\sigma/dx_p$ as function of the square of the c.m. energy $s = W^2$. The curves show fits of the form $1 + c_1 \ln (s/1\text{GeV}^2)$.

Fig. 4 Inclusive charged particle production. Coefficients c_1 (see curves in Fig. 3) as function of x_p as measured by TASSO and PLUTO.

Fig. 5 $D^{*\pm}$ production. Distribution of the difference of the invariant masses $\Delta M = M(K^-\pi^+\pi^+) - M(K^-\pi^+)$ for $M(K^-\pi^+)$ masses in the D^0 mass region, and for $x > 0.5$. The charge conjugated combinations are included.

Fig. 6 $D^{*\pm}$ production. Scaled cross section $s\, d\sigma/dx$ as function of $x = E_{D^*} / E_{beam}$.

Fig. 7 $D^{*\pm}$ production. Distribution of the production angle $\cos\theta_{D^*}$ for $x > 0.5$. The curves are fits of the form $1 + a\cos\theta + \cos^2\theta$ (full curve) and $1 + \cos^2\theta$ (dashed curve).

Fig. 8 Lepton pair production. Differential cross section $d\sigma/d\Omega$, divided by the QED cross section, for pair production of e^+e^-, $\mu^+\mu^-$, $\tau^+\tau^-$.

Fig. 9 Search for charged Higgs and technipions. Limits on the hadronic branching ratio (B_{had}) as function of mass m_H. Also shown are the limits on the leptonic branching ratio ($B_{\tau\nu}$) as obtained by the JADE experiment.

Fig. 10 Production of f'(1515)

a) Distribution of the invariant mass $M(K^+K^-)$. The full curve is the result of a fit with interfering contributions from f^0, A_2 and f', and a background. The dotted curve shows the contributions from f^0, A_2 and f'. The background contribution is given by the dashed line.

b) Distribution of the invariant mass $M(K_S^0 K_S^0)$. The full curve is the result of a fit with interfering contributions from f^0, A_2, and f', and a background (dashed line).

Fig. 11 Reaction $\gamma\gamma \to \pi^+\pi^-\pi^+\pi^-$. Distribution of the four pion mass $M_{4\pi}$. The curve shows the result of a fit of a Breit-Wigner plus a smooth background.

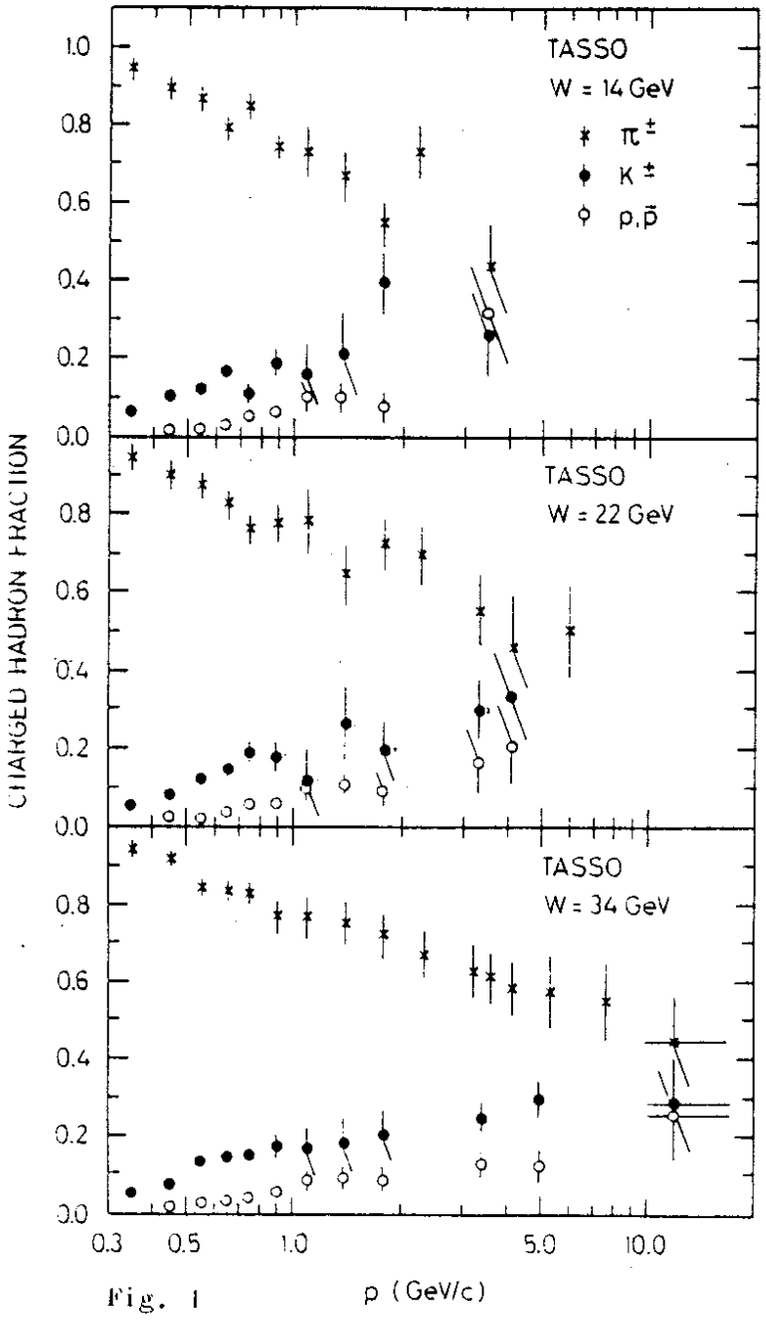
TASSO
W = 14 GeV
π±
K±
p,p̄
TASSO
W = 22 GeV
TASSO
W = 34 GeV
CHARGED HADRON FRACTION
p (GeV/c)
0.3
0.5
1.0
5.0
10.0

Fig. 1

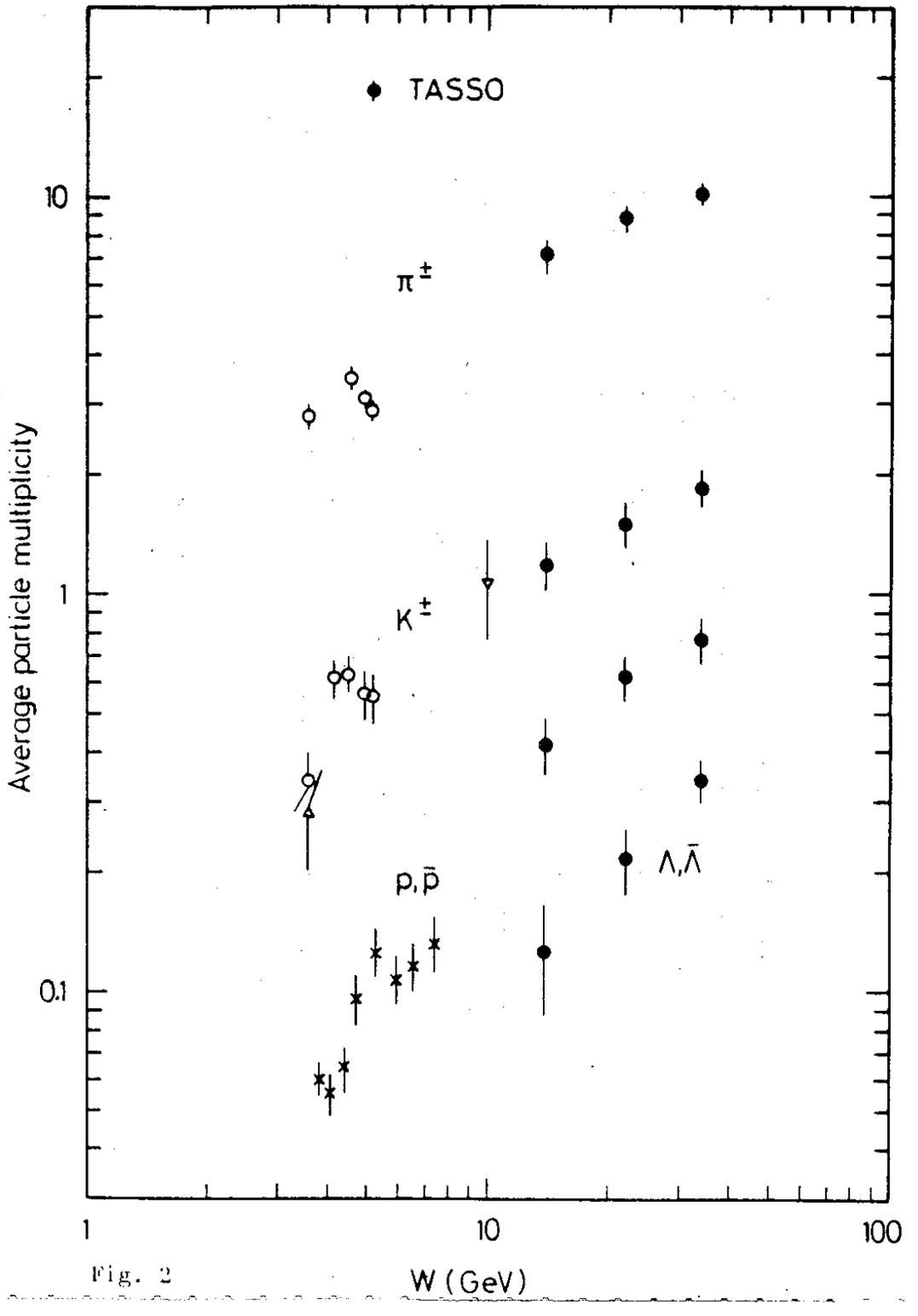
TASSO
π±
K±
p,p̄
Λ,Λ̄
Average particle multiplicity
W (GeV)
1
10
100
0.1

Fig. 2

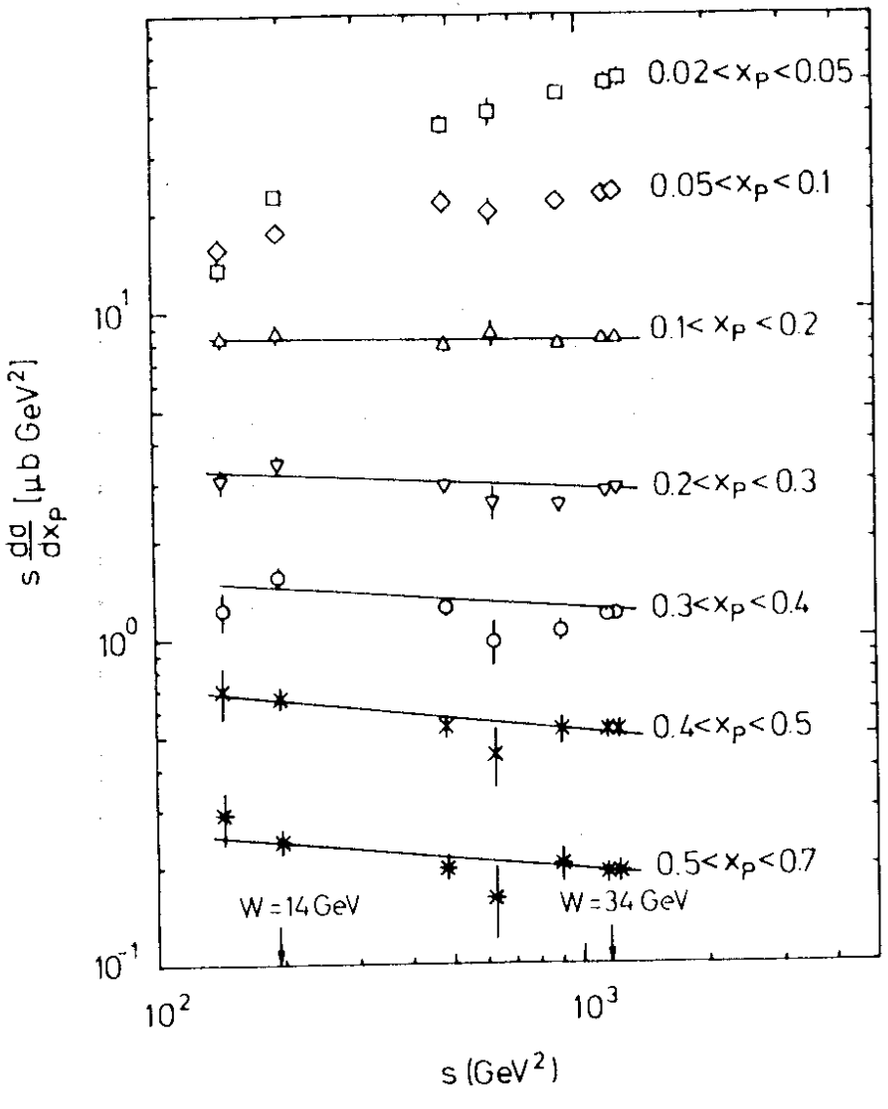
0.02<xp<0.05
0.05<xp<0.1
0.1<xp<0.2
0.2<xp<0.3
0.3<xp<0.4
0.4<xp<0.5
0.5<xp<0.7
W=14 GeV
W=34 GeV
s dσ/dxp [μb GeV²]
s (GeV²)

Fig. 3

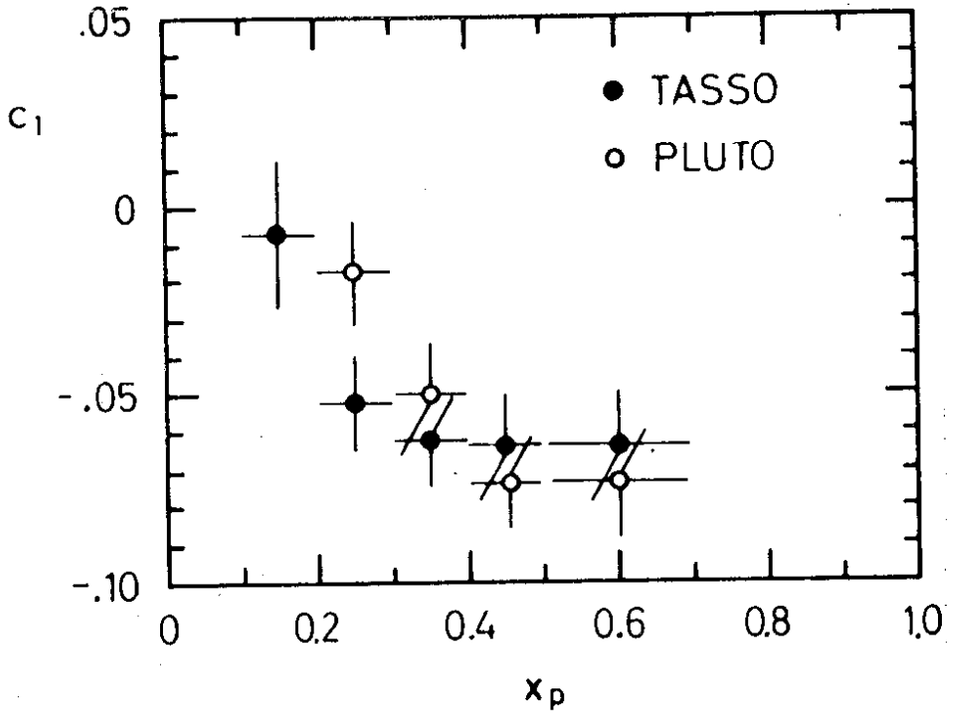
TASSO
PLUTO
c1
xp

Fig. 4

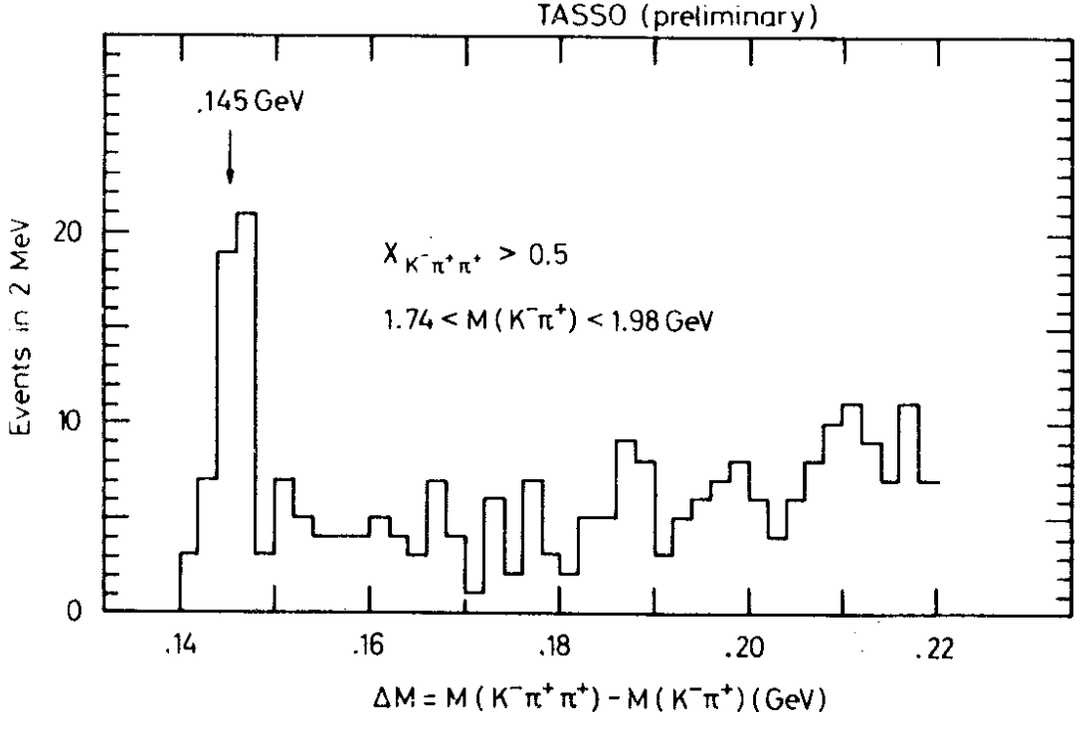

Fig. 5

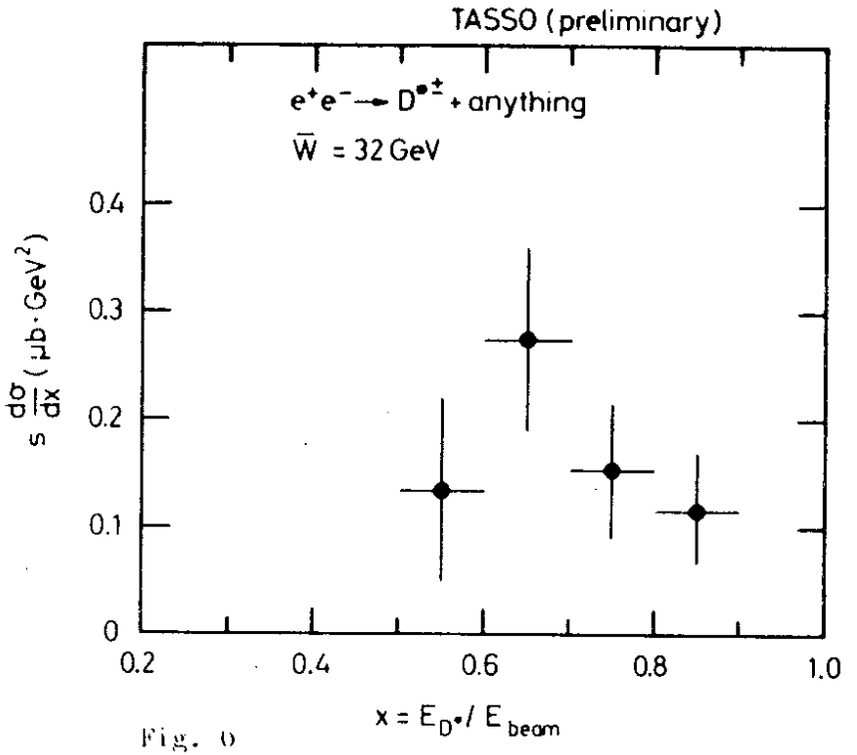

Fig. 6

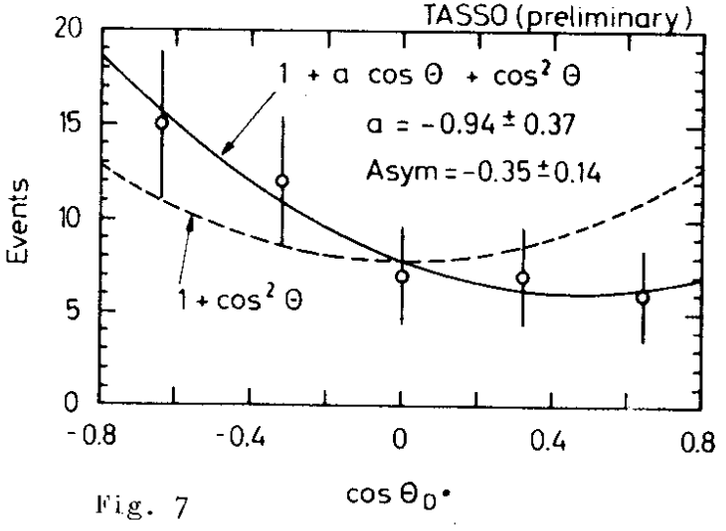

Fig. 7

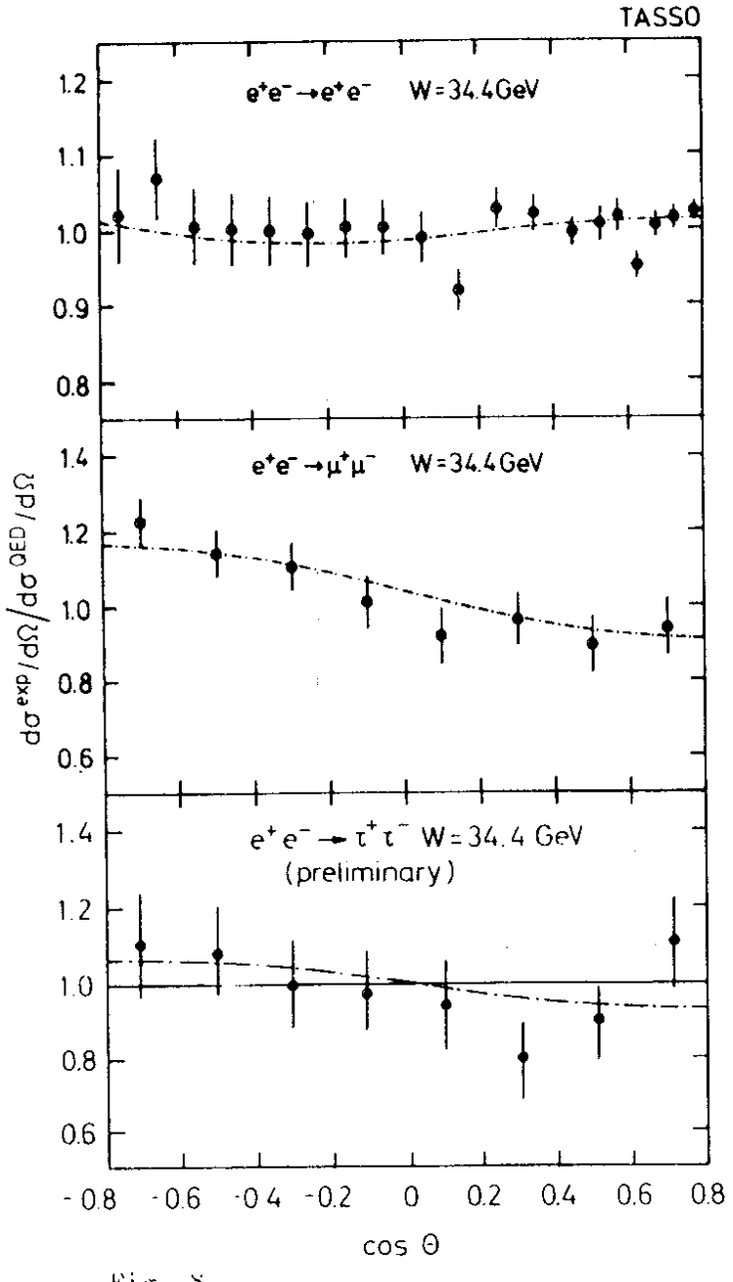
TASSO
e⁺e⁻→e⁺e⁻ W=34.4GeV
e⁺e⁻→μ⁺μ⁻ W=34.4GeV
e⁺e⁻→τ⁺τ⁻ W=34.4 GeV
(preliminary)
dσ^exp/dΩ/dσ^QED/dΩ
cos Θ

Fig. 8

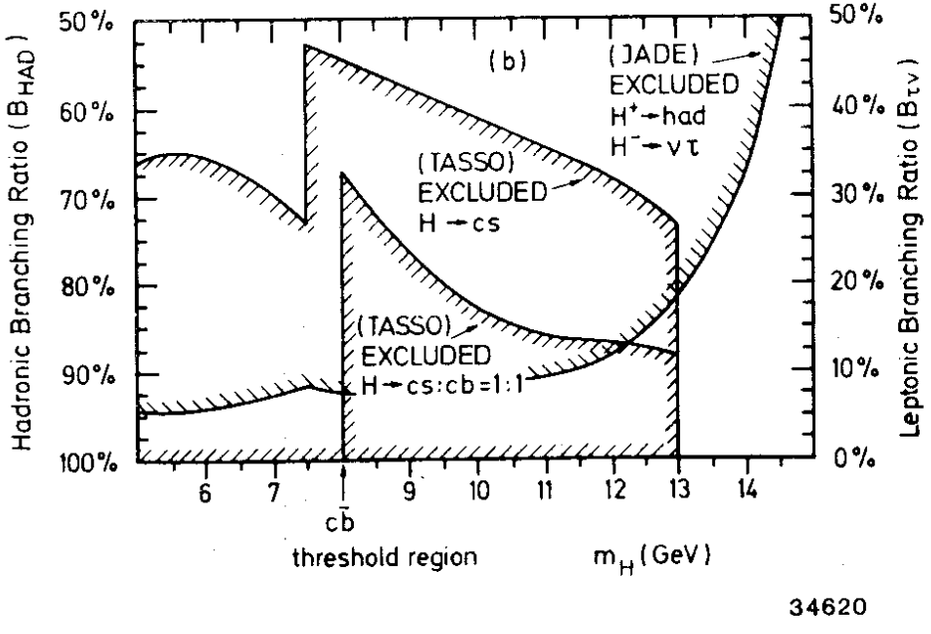
(b)
(JADE)
EXCLUDED
H⁺→had
H⁻→ντ
(TASSO)
EXCLUDED
H→cs
(TASSO)
EXCLUDED
H→cs:cb=1:1
Hadronic Branching Ratio (B_HAD)
Leptonic Branching Ratio (Bτν)
cb̄
threshold region
m_H (GeV)
34620

Fig. 9

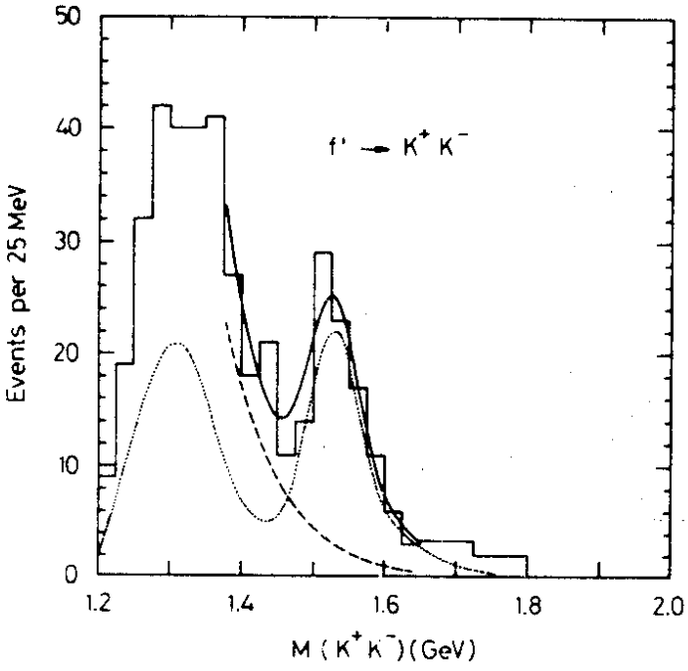

Fig. 10a

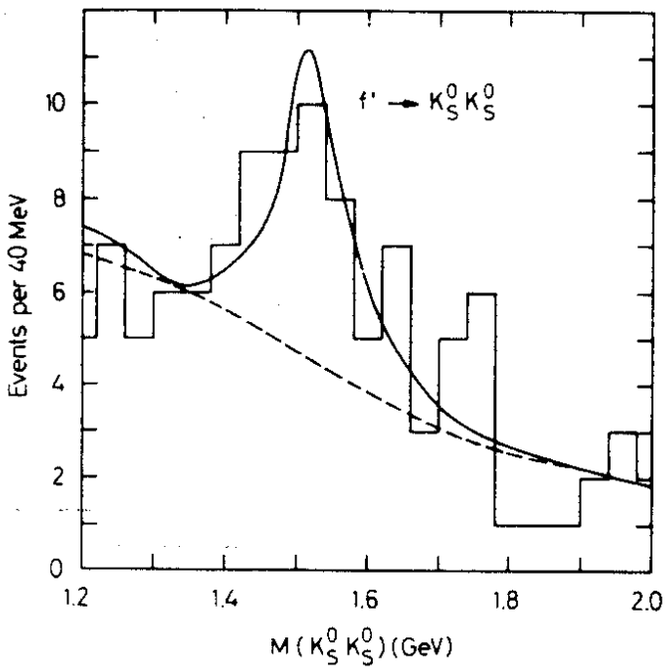

Fig. 10b

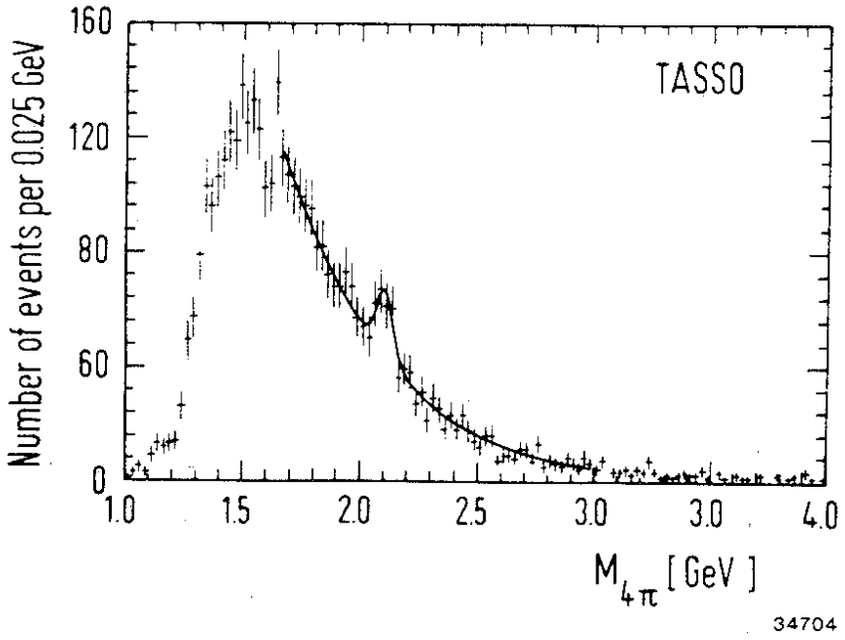

Fig. 11